International Journal of Mechanical and Electrical Engineering
ISSN: 3005-9615 (Print), ISSN: 3005-7132 (Online) | Volume 8, Number 3, Year 2026
DOI: https://doi.org/10.62051/ijmee.v8n3.01
Journal homepage: https://wepub.org/index.php/IJMEE/index

Research on the Influence of Cycloid Gear Installation Deviation on Tooth Surface Error

Qinglei Wei *

School of Mechanical Engineering, Tianjin University of Technology and Education, Tianjin, 300350, China

* Corresponding Author Email: 1564848064@qq.com

ABSTRACT

To investigate the influence of workpiece-tool position errors on the tooth surface during the grinding of RV reducer cycloidal gears using a worm wheel, the study is based on meshing theory. Starting from the tooth profile equation of the worm wheel's normal cross-section, the meshing equation for grinding cycloidal gears with the worm wheel is derived. By introducing coordinate transformation matrices that account for installation angle deviations of the worm wheel, eccentricity of the cycloidal gear workpiece, and flatness deviations, the tooth surface equation of the cycloidal gear under error conditions is calculated. The correctness of the theory and analysis is verified through VERICUT grinding simulation. Through comparative analysis, the impact patterns of various errors on the tooth surface are obtained, which can provide a theoretical basis for error compensation in the grinding of cycloidal gears.

KEYWORDS

Worm Wheel; Cycloidal Gear; Error Analysis; Tooth Surface Deviation.

1. INTRODUCTION

Continuous generating grinding technology, characterized by its high precision and efficiency, has become a crucial technique in the field of precision gear machining, particularly well-suited for the machining of gears with continuous tooth profile curves, such as cycloidal gears in RV reducers. Litvin[1] et al. derived the general equation for the helical surface of worm gears and the meshing equation with the tooth surface of worm wheels based on differential geometry and spatial meshing theory. They studied the meshing characteristics of double-enveloping worm gears and achieved contact analysis of the two tooth surfaces through computer simulation. In the process research on worm grinding wheel grinding of helical gears, Wu Yanming[2] et al. proposed applying tangential differential cutting technology to gear grinding machines with non-differential structures, which not only improved the machining accuracy of the machine tool but also expanded its machining capabilities. Chen Qidi[3] et al. systematically summarized the research status and development trends of error compensation technologies in ultra-precision machining, emphasizing the significant impact of geometric errors, force-induced errors, and thermal-induced errors on ultra-precision machining, as well as the corresponding compensation methods. Li Shiping[4] et al. developed a general kinematic error decoupling model applicable to any multi-axis CNC machine tool. This model can describe the dynamic variation laws of machine tool errors and support real-time compensation of errors in the working area. Yang Jianguo[5] et al. used the homogeneous coordinate transformation method to establish a generalized model for volumetric errors in multi-axis machine tools and designed a general error compensation scheme for four types of machining centers, ultimately achieving efficient compensation of machine tool errors through high-speed Ethernet. Zhang Wanli[6] simplified the model under the assumption of small errors based on multi-body system theory and the principle of standard homogeneous coordinate transformation, constructing a comprehensive mathematical model for the spatial geometric errors of CNC machine tools. Tao Xiaohui[7] et al. proposed a geometric error sensitivity analysis method combining screw theory and the Sobol method to identify key error terms affecting the spatial accuracy of worm grinding wheel gear grinding machines. Additionally, Zhang Minghui[8] designed a comprehensive radial and tangential compensation method based on the grinding principle of CNC cycloidal gear forming gear grinding machines. Pang Yuan[9] proposed a segmented modification design method for optimizing the tooth profile of cycloidal gears and conducted in-depth research on their continuous generating grinding process. Han Feilong[10] et al. established a mathematical model for worm grinding wheel gear grinding based on worm grinding wheel tooth profile reverse engineering technology. According to the dual-parameter meshing principle, they derived the tooth surface shape of the worm grinding wheel inversely from the modified tooth surface of the gear. Through projection transformation, the contact trace lines on the grinding wheel tooth surface were converted into axial section tooth profile curves, and the influence of variations in parameters such as the number of heads and radius of the worm grinding wheel on the grinding wheel profile, shaft intersection angle, and meshing trace lines was further discussed, systematically analyzing the influence laws of different parameters on generating gear grinding.

During precision grinding processes, due to insufficient machining accuracy of machine tool components and cumulative assembly errors, coupled with mechanical deformations caused by cutting forces and cutting heat, positional deviations occur between the actual machining coordinate system of the machine tool and the theoretical model. These deviations accumulate through the transmission of the machine tool's kinematic chain and ultimately manifest as relative positional errors between the grinding wheel and the workpiece. Specifically, in the machining process of worm grinding wheel grinding of cycloidal gears, the main sources of positional errors include key parameters such as eccentric installation errors of the workpiece, end face flatness deviations, and installation angle errors of the tool axis system.

Building upon previous research, this paper focuses on the worm grinding wheel grinding of cycloidal gears and analyzes the influence of positional errors between the workpiece and the tool on tooth surface accuracy during the worm grinding wheel grinding process of RV reducer cycloidal gears based on meshing principles. Firstly, a meshing mathematical model for the grinding of cycloidal gears is established according to the tooth profile equation of the normal section of the worm grinding wheel. An error tooth surface equation incorporating error factors is constructed through error coordinate transformation matrices. To verify the accuracy of the theoretical model, mainstream cutting simulation machining is employed for validation. Based on the computational results, the influence laws of different errors on tooth surface formation are systematically revealed, providing theoretical support for error compensation in subsequent precision grinding of cycloidal gears.

2. CYCLOIDAL GEAR GENERATING MACHINING MODELING

2.1. Worm Wheel Tooth Surface Equation and Coordinate System Establishment

The shape of the grinding wheel can be derived from the tooth profile of the gear shaper cutter, that is, the tooth profile curve of the grinding wheel's normal section is obtained through helical motion. The equation [12] for the normal tooth profile is

$$r_n = [x_n \quad 0 \quad z_n \quad 1] \tag{1}$$

Specifically

$$
\begin{gathered}
x_n = R_{eb} + r_z\cos(\gamma+\varphi) - R_z\cos(c_1) + A\cos(\varphi-u) + R_{dj} \\
z_n = R_{eb}\varphi + r_z\sin(\gamma+\varphi) - R_z\sin(c_1) + A\sin(\varphi-u) \\
\gamma = \arctan\left(\frac{\left(A\sin u - \frac{R_Z}{Z_Z}\sin\left(\frac{u}{Z_Z}\right)\right)}{\frac{R_Z}{Z_Z}\cos\left(\frac{u}{Z_Z}\right) - A\cos u}\right) \\
\varphi = \frac{\pi}{2} - \gamma - \arccos(c_2) \\
c_1 = \varphi - \frac{u}{Z_z} \\
c_2 = \frac{\left(R_Z\sin\left(\frac{u}{Z_Z}+\gamma\right) - A\sin(u+\gamma)\right)}{R_{eb}}
\end{gathered}
\tag{2}
$$

In the formula, u represents the equation parameter, R_z denotes the radius of the pin gear distribution circle, Z_z signifies the number of pin gear teeth, A stands for the eccentricity, R_{eb} indicates the radius of the cycloid gear tooth tip circle, r_z represents the radius of the pin gear, and R_{dj} represents the pitch circle radius of the grinding wheel.

$$
\begin{gathered}
r_1 = M_{wn} r_n \\
M_{wn} = \begin{bmatrix} \cos(\theta+\theta_0) & -\sin(\theta+\theta_0) & 0 & 0 \\ \sin(\theta+\theta_0) & \cos(\theta+\theta_0) & 0 & 0 \\ 0 & 0 & 1 & \frac{T\theta}{2\pi} \\ 0 & 0 & 0 & 1 \end{bmatrix} \\
T = \frac{2\pi R_{gj}}{Z_b\cos\lambda}
\end{gathered}
\tag{3}
$$

In equation (3), r_1 represents the parameter expression of the grinding wheel equation. In the equation, T denotes the lead, R_{gj} signifies the pitch radius of the cycloidal gear, Z_b indicates the number of teeth of the cycloidal gear, and λ represents the helix angle of the grinding wheel. Based on the meshing principle, the tooth surface equation of the cycloidal gear can be derived through homogeneous coordinate transformation, and the meshing equation is as follows:

$$
\begin{cases} f = v_{12}\cdot n = 0 \\ r_2 = M_{21}\cdot r_1 \end{cases}
\tag{4}
$$

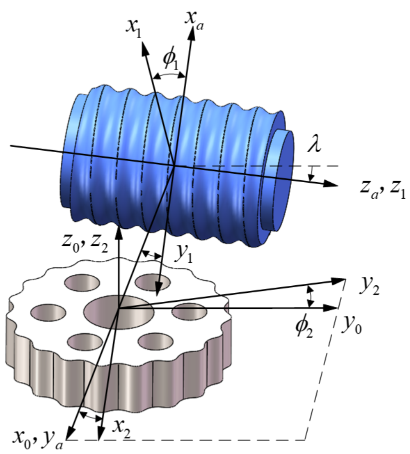

Figure 1. Schematic diagram of coordinate system for cycloid wheel grinding

The relationship between ϕ_1 and u and θ can be obtained through formula (4). By gradually changing the value of u at a certain step length, a series of points on the tooth profile of the cycloid wheel's grinding wheel end face can be traversed, and the meshing points on the grinding wheel can be obtained. Through matrix transformation to the cycloid wheel, the meshing trajectory can be obtained.

2.2. Establishment of Tooth Surface Error Model for Gear Grinding

Due to positioning assembly or rough machining accuracy, the rotation axis of the workpiece is not in the theoretical position, resulting in a deviation, as shown in Figure 2. Let the eccentric offset of the workpiece be δ_d, which is the distance between the origin of the theoretical coordinate system of the workpiece and the actual coordinate system. The angle between the line connecting the two origins and the y-axis is γ. At this time, the pose error of the workpiece is as shown in the figure, which is equivalent to introducing a coordinate transformation matrix containing the offset δ_d and the angle γ.

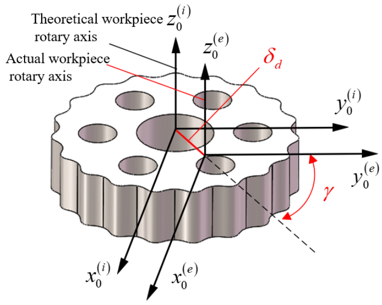

Figure 2. Schematic diagram of eccentricity of cycloid gear workpiece

$$E_d = \begin{bmatrix} 1 & 0 & 0 & \delta_d\cos\gamma \\ 0 & 1 & 0 & \delta_d\sin\gamma \\ 0 & 0 & 1 & 0 \\ 0 & 0 & 0 & 1 \end{bmatrix} \quad (5)$$

When installing the cycloidal gear workpiece, inaccuracies in positioning or insufficient machining precision of the roughcast reference surface can lead to deflection errors on the horizontal plane, also known as flatness errors, as illustrated in Figure 3.

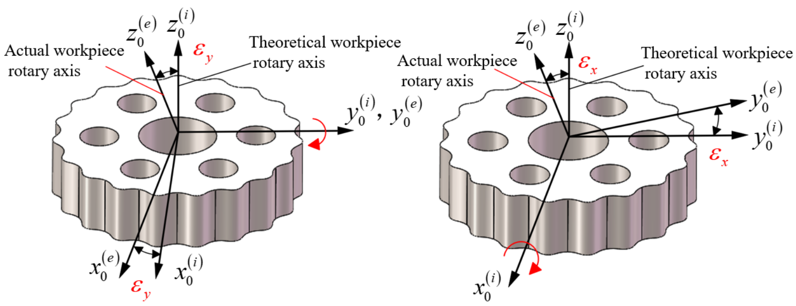

Figure 3. Schematic diagram of planeness error of cycloidal gear workpiece

$$E_y = \begin{bmatrix} \cos\varepsilon_y & 0 & \sin\varepsilon_y & 0 \\ 0 & 1 & 0 & 0 \\ -\sin\varepsilon_y & 0 & \cos\varepsilon_y & 0 \\ 0 & 0 & 0 & 1 \end{bmatrix}$$
$$E_x = \begin{bmatrix} 1 & 0 & 0 & 0 \\ 0 & \cos\varepsilon_x & \sin\varepsilon_x & 0 \\ 0 & -\sin\varepsilon_x & \cos\varepsilon_x & 0 \\ 0 & 0 & 0 & 1 \end{bmatrix} \quad (6)$$

Let the deflection angles in the x-axis and y-axis directions be denoted as ε_x and ε_y, respectively. Similarly, two coordinate transformation matrices containing the deflection angles ε_x and ε_y are introduced to obtain the equation of the error tooth surface.

The grinding wheel installation angle error refers to the deviation of the angle between the axis of the grinding wheel tool and the axis of the cycloidal wheel workpiece from the design angle. Let the deviation angle be ε_a. The schematic diagram of the grinding wheel installation angle error is shown in Figure 4.

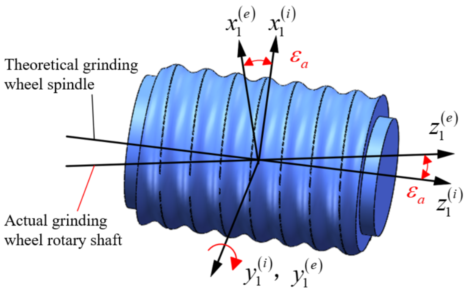

Figure 4. Schematic diagram of worm wheel installation angle error

When there is a tilt error in the grinding wheel, the corresponding coordinate transformation matrix is as follows:

$$E_a = \begin{bmatrix} \cos\varepsilon_a & 0 & -\sin\varepsilon_a & 0 \\ 0 & 1 & 0 & 0 \\ \sin\varepsilon_a & 0 & \cos\varepsilon_a & 0 \\ 0 & 0 & 0 & 1 \end{bmatrix} \tag{7}$$

The expression for the error tooth surface is

$$\begin{cases} f = v_{12} \cdot n = 0 \\ r_2^{(e)} = M_{21}^{(e)} \cdot r_1 \end{cases} \tag{8}$$

in the formula

$$\begin{gathered} M_{21}^{(e)} = M_{20}^{(e)} M_{0a}^{(e)} M_{a1} \\ M_{0a}^{(e)} = M_{0a} E_a \\ M_{20}^{(e)} = M_{20} E_d E_x E_y \end{gathered} \tag{9}$$

Given the rotational angle ϕ_1 of the grinding wheel, the coordinates of the contact points on the gear tooth surface can be obtained both without error and under the influence of gear grinding error.

When there is no error, the unit normal vector of the tooth surface contact point is represented as

$$n_2^{(i)}(\phi_1) = -M_{21}(\phi_1) n_1(u, \theta) \tag{10}$$

The negative sign in the formula is to make the unit normal vector of the tooth surface contact point point outward from the gear body. The normal error $\delta_{2n}(\phi_1)$ of the tooth surface corresponding to this tooth surface contact point as

$$\begin{gathered} r_2^{(i)}(\phi_1) = M_{21}(\phi_1) r_1(u, \theta) \\ r_2^{(e)}(\phi_1) = M_{21}^{(e)}(\phi_1) r_1^{(e)}(u, \theta) \\ \delta_{2n}(\phi_1) = \left(r_2^{(e)}(\phi_1) - r_2^{(i)}(\phi_1) \right) \cdot n_2^{(i)}(\phi_1) \end{gathered} \tag{11}$$

The schematic diagram of normal error $\delta_{2n}(\phi_1)$ is shown in Figure 5, and a calculation analysis is conducted in conjunction with a machining example.

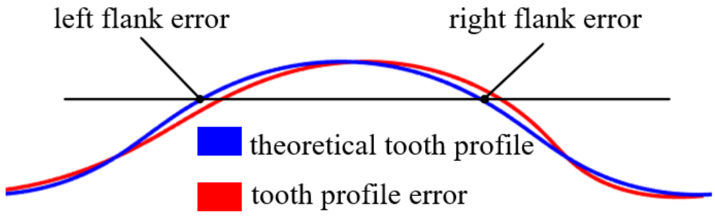

Figure 5. Schematic diagram of normal error of tooth profile

3. ERROR RESULT ANALYSIS

Using MATLAB software, it is possible to simultaneously plot theoretical tooth profiles and actual tooth profile models. Subsequently, the normal error of the meshing point tooth surface of the cycloidal gear can be calculated, and the pattern of tooth profile errors of the cycloidal gear can be analyzed. The following results were obtained through MATLAB calculations.

Analysis of tooth profile error caused by the installation angle offset ε_a. When the offset ε_a of the grinding wheel deflecting around the y-axis is -0.01 or 0.01 rad, the error tooth profiles of the left and right tooth surfaces are shown in Figure 6. Changes in the installation angle will cause variations in the tooth thickness of the tooth surface, and both positive and negative deviations of the installation angle result in a decrease in the tooth thickness of the tooth surface. The changes in tooth thickness at the tooth tip and tooth root are minimal, while the decrease in tooth thickness is greatest near half the tooth height. Meanwhile, there is almost no error variation in the tooth width direction, with the maximum calculated error being -0.0002 mm and the minimum being -0.0081 mm.

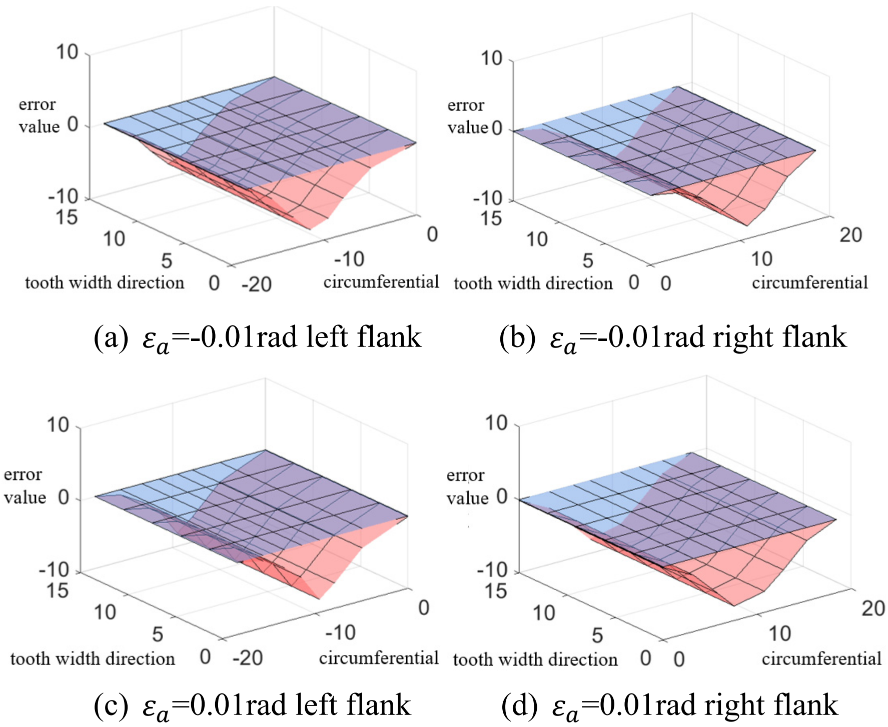

Figure 6. Tooth profile under installation angle offset

Analysis of tooth profile error caused by the y-axis deflection of the workpiece, resulting in an offset ε_y. When the cycloid gear workpiece rotates around the y-axis with a deflection angle ε_y of -0.01 and 0.01 rad, the error tooth profiles of the left and right tooth surfaces are shown in Figure 7. When ε_y is less than 0, the tooth thickness of the tooth surface changes. Starting from the upper surface of the gear, the error value gradually decreases in the direction of the tooth width. The maximum error value calculated is 0.036 mm, and the minimum value is -0.006 mm. When ε_y is greater than 0, the error value gradually increases in the direction of the tooth width. Both positive and negative deviations around the y-axis result in an increase in the tooth thickness of the tooth surface, with only a small portion of the tooth thickness decreasing. The error value changes consistently, but the trends are exactly opposite. Meanwhile, the error changes slightly in the circumferential direction.

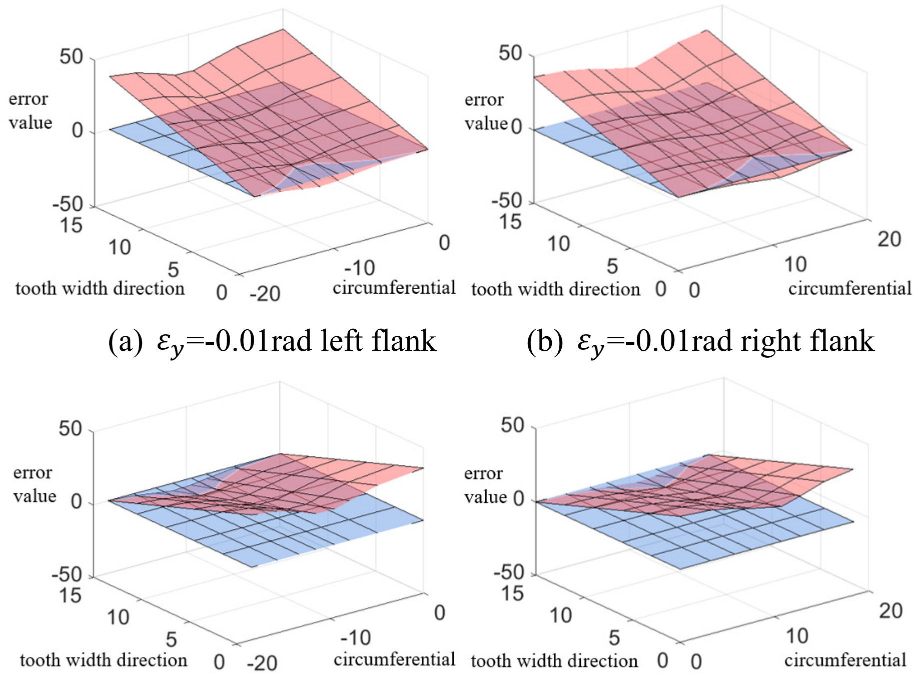

(a) ε_y=-0.01rad left flank (b) ε_y=-0.01rad right flank

(c) ε_y=0.01rad left flank (d) ε_y=0.01rad right flank

Figure 7. Tooth profile under the condition of workpiece offset around the y-axis

Analysis of tooth profile error caused by axial deflection of the workpiece. When the cycloid gear workpiece rotates around the axis with a deflection angle ε_x of -0.01 and 0.01 rad, the error tooth profiles of the left and right tooth surfaces are shown in Figure 8. When ε_x is less than 0, the maximum error value is calculated to be 0.0312 mm, and the minimum error value is -0.0312 mm. The error variation trends of the left and right tooth surfaces are similar, starting from the upper surface of the gear, with the absolute value of the error gradually increasing in the tooth width direction, and the variation is greater near the half-height point of the tooth. When ε_x is greater than 0, the maximum error value is calculated to be 0.0312 mm, and the minimum error value is -0.0312 mm. The error variation trends of the left and right tooth surfaces are similar, starting from the upper surface of the gear, with the absolute value of the error gradually increasing in the tooth width direction, and the variation is greater near the half-height point of the tooth. Additionally, the error results brought by positive and negative deviations of ε_x are exactly opposite.

Analysis of tooth profile error caused by workpiece eccentricity. When the eccentricity of the cycloid gear workpiece has an eccentric distance δ_a=0.05mm and the eccentric angles γ are 0°, 30°, 60°, and 90°, the error tooth profiles of the left and right tooth surfaces are shown in Figure 9. Changes in the eccentric position will cause variations in the tooth thickness of the tooth surface. As the eccentric angle gradually increases from 0° to 90°, the impact on the tooth profile changes is concentrated at half the tooth height, transitioning from maximum to minimum, with the influence on tooth thickness increasing from small to large. Meanwhile, there is almost no error variation in the tooth width direction. At 0°, the maximum error value is 0.0371mm, and the minimum is -0.0371mm. By calculating equation (8) using MATLAB, the impact of other eccentric angles on the cycloid gear tooth surface can be obtained. Compared to the impact pattern of the tooth surface as the eccentric angle varies from 0° to 90°, the trend is the same when changing from 180° to 90°, but the tooth profile changes are opposite. When changing from 180° to -90°, both the trend and tooth profile changes are opposite. When changing from 0° to -90°, the trend changes, but the tooth profile changes are consistent.

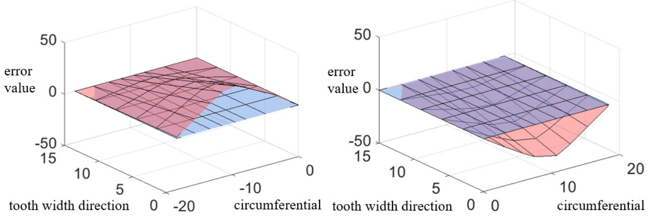

(a) ε_x=-0.01rad left flank (b) ε_x=-0.01rad right flank

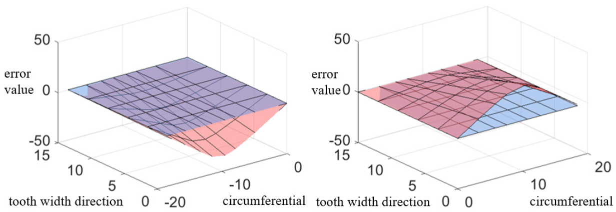

(c) ε_x=0.01rad left flank (d) ε_x=0.01rad right flank

Figure 8. Tooth profile under the condition of workpiece offset around the x-axis

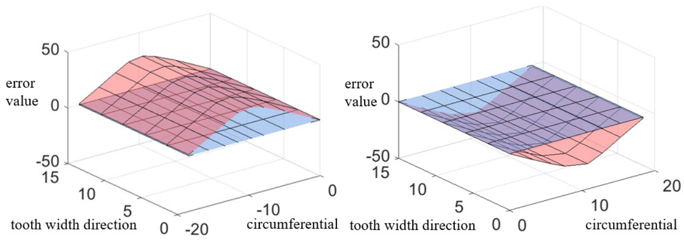

(a) γ=0 left flank (b) γ=0 right flank

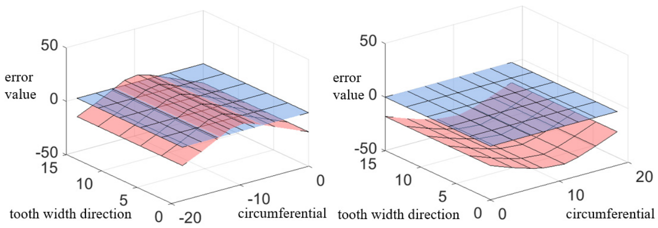

(c) γ=30° left flank (d) γ=30° right flank

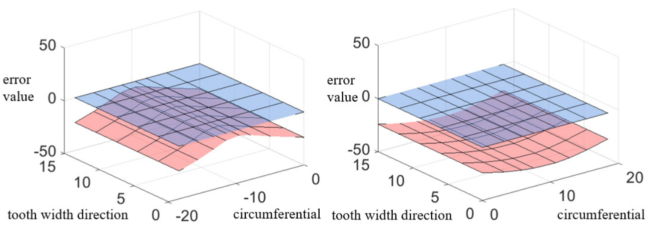

(e) γ=60° left flank (f) γ=60° right flank

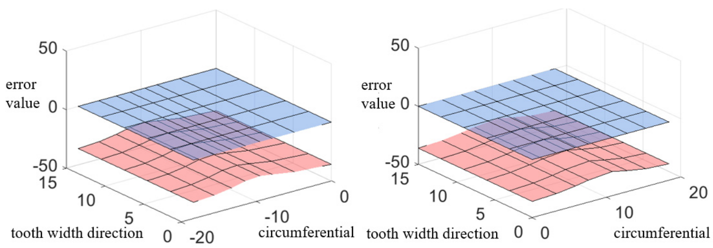

(g) γ=90° left flank (h) γ=90° right flank

Figure 9. Tooth profile under workpiece eccentricity

4. SIMULATION ANALYSIS OF CYCLOID GEAR GRINDING

To verify the accuracy of the analysis on the impact of machining errors on tooth surfaces mentioned earlier, the VERICUT simulation machining software was used to simulate the grinding of cycloidal gears using a worm wheel grinding wheel. A simplified machining model was established based on the kinematic structure of the worm wheel gear grinding machine, as shown in Figure 10. During machining, the spindle and workpiece shaft maintain a certain center distance and speed ratio while rotating, and then the tool moves in the Z-axis direction to machine the tooth width of the cycloidal gear.

During the simulation process, if no positional deviation is introduced, the theoretical tooth surface can be obtained. If positional deviation is set, the tooth surface with positional deviation can be obtained. At the same time, by utilizing the automatic comparison function in VERICUT, as long as the theoretical tooth surface is imported into the design, a comparison between the theoretical and error tooth surfaces can be obtained. For example, setting A to 3.573 in the machining program can result in an A-axis deflection angle of 0.01 rad, and at this time, the machining can produce the tooth surface under error conditions.

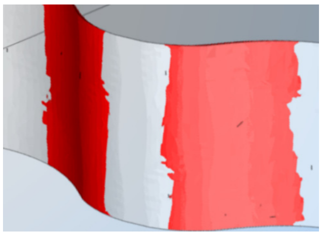

Figure 10. Simulation result of grinding wheel installation angle error

As shown in the figure, the automatic comparison results of the simulated machining are consistent with the analysis and comparison of the tooth surface variation pattern of the installation angle error mentioned earlier. The overcutting is concentrated at half the tooth height. The red part indicates overcutting, while the blue part indicates residuals. Additionally, the error value can be obtained by analyzing the tool to "measure the distance between the blank and the design". The average error value of a series of points measured at half the tooth height is -0.0079mm, which deviates by 2.47% from the error value calculated earlier.

Using the same rotation and movement of the blank function, the error simulation results of workpiece eccentricity and deflection are as follows. The comparison diagrams of tooth surfaces are set with the blank deflected along the y-axis by ε_x=0.01rad and δ_d=0.05mm, respectively, and γ=0. When ε_x=0.01rad, as shown in Figure 11, there is residual on the lower part of the left tooth surface, and overcutting on the lower part of the right tooth surface. The automatic comparison results of the simulated machining are consistent with the analysis and comparison of the tooth surface variation pattern for ε_x error mentioned earlier, with a maximum error of 0.0326mm, which deviates by 4.48% from the error value calculated earlier. When δ_d=0.05mm and γ=0, as shown in Figure 12, there is residual on the entire left tooth surface, and overcutting on the right tooth surface. The automatic comparison results of the simulated machining are consistent with the analysis and comparison of the tooth surface variation pattern for eccentricity error mentioned earlier, with a maximum error of 0.0352mm, which deviates by 5.12% from the error value calculated earlier.

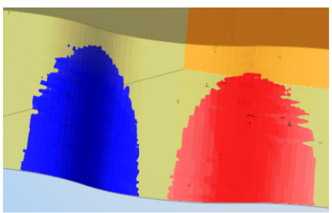

Figure 11. Simulation result of workpiece flatness error

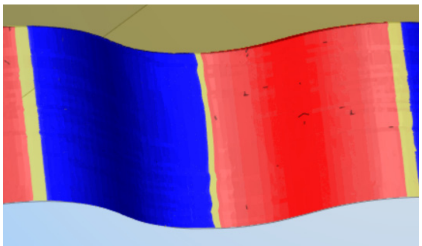

Figure 12. Simulation result of workpiece eccentricity error

In summary, through simulation analysis of the previous examples, the correctness of the analysis and theoretical model has been verified.

5. SUMMARY

Based on the meshing principle, this article establishes a mathematical model that starts from the normal section profile of the worm wheel grinding wheel and proceeds to the error tooth surface of the cycloidal wheel. It analyzes the influence patterns of grinding wheel installation angle errors, as well as eccentricity and deflection errors of the cycloidal wheel workpiece, on the tooth surface. The correctness of the analysis results and theoretical model is verified through simulation machining using VERICUT, and the following conclusions are drawn.

The four types of deviations studied have different forms and patterns of impact on the tooth surface. The installation angle deviation ε_a leads to a reduction in tooth thickness with no change in the tooth width direction. The deviation ε_y around the y-axis of the workpiece causes the tooth thickness to gradually increase or decrease in the tooth width direction. The deviation ε_x around the x-axis leads to a gradual increase or decrease in tooth thickness in the tooth width direction, with opposite error values on the left and right tooth surfaces. The variation in the tooth height direction is first increasing and then decreasing. The closer the eccentric position of the workpiece is to the y-axis, the greater the difference in variation between the left and right tooth surfaces. The closer it is to the x-axis, the more significant the simultaneous impact on the tooth thickness of both the left and right tooth surfaces.

In actual machining, error factors do not occur individually but generally coexist. Based on the error detection results of the machined cycloid gear and the influence pattern of errors, the main influencing factors are identified. According to these factors, the corresponding numerical control program or the positions of the worm wheel and cycloid gear workpieces are adjusted to obtain a cycloid gear with higher precision.

REFERENCES

[1] Litvin F L, Fuentes A. Gear geometry and applied theory[M]. Cambridge University Press,2004.

[2] Wu, Y. M., Han, J., Wang, C. X., et al. Deep-cut and creep-feed grinding on worm grinding wheel gear grinding machine [J]. Machinery Manufacturing, 2000, (07): 31-32.

[3] Chen, Q. D., Hu, X. L., Lin, M., et al. A review of research on error compensation technology in ultra-precision machining [J]. China Mechanical Engineering, 2023, 34(03): 253-268.

[4] Su, S. P., Li, S. Y. Kinematic modeling of multi-body system for comprehensive spatial errors of five-axis CNC machine tools [J]. Combined Machine Tool and Automatic Machining Technology, 2003, (05): 17-20+23.

[5] Xiang, S. T., Du, Z. C., Yang, J. G. New progress in research on measurement and modeling of geometric and thermal errors of CNC machine tools [J]. Machine Design and Research, 2019, 35(06): 52-57.

[6] Zhang, W. L. Geometric error modeling of the whole five-axis CNC gear grinding machine and machine tool accuracy design [D]. Xi'an University of Technology, 2018.

[7] Tao, X. H., Li, G. L., Xu, K., et al. Sensitivity analysis of geometric errors of worm grinding wheel gear grinding machine [J]. Chinese Journal of Engineering Design, 2020, 27(01): 111-120.

[8] Zhang, M. H., Deng, X. Z., Su, J. X. Influence of eccentricity on forming grinding of cycloidal gears and its compensation [J]. Journal of Mechanical Transmission, 2021, 45(07): 12-17.

[9] Pang, Y. Research on segmented modification design of cycloidal gears and its continuous generating grinding process technology [D]. Chongqing University, 2021.

[10] Han, F. L. Research on tooth profile reverse engineering and dressing grinding wheel profile calculation method of worm grinding wheel for generating gear grinding [D]. Henan University of Science and Technology, 2023.

[11] Han, F. L., Yang, J. J., Wang, S., et al. Influence of worm grinding wheel position changes on tooth surface deviations in generating gear grinding [J]. Tool Engineering, 2024, 58(02): 60-65.

[12] Zhuang, Z. Y., Wang, C. Y. Calculation of tooth profile of cycloidal gear hob using tooth profile normal method [J]. Tool Engineering, 1979, (06): 50-52.

[13] Ren, L. Research on geometric error mapping and compensation of large-scale CNC gear hobbing machine tools [D]. Chongqing University, 2019.